

# Electrical Characterization of Rolls and Belts for High Speed Electrophotography

Ming-Kai Tse and Inan Chen; Quality Engineering Associates (QEA), Inc.; Burlington, MA, USA

## Abstract

The performance of rolls and belts used in charging, development and transfer processes of electrophotography depends critically on dielectric relaxation of the semi-insulating overcoat layers. In these materials, the time rate of dielectric relaxation is shown to be determined by charge injection from the bias and charge mobility, rather than by the bulk resistance. Thus, characterization of these devices, especially in high-speed printing applications, where time allotted for each process becomes limited, should emphasize the transient characteristics and spatial variations of dielectric relaxation.

## Introduction

In electrophotography (EP), rolls and belts are used in development and transfer of toners, as well as to charge photoreceptors. These processes involve electrical forces and hence, the electrical properties of these devices are expected to play important roles in their performance. Apparently, the simplest electrical property for characterizing rolls and belts is the resistance. However, measurements of steady-state resistance have been poor in reproducibility and/or inconsistent with the device performance.

The rolls and belts consist of a conductive substrate overcoated with more resistive, semi-insulating dielectric layer. The progress of these EP processes is controlled by dielectric relaxation in this overcoat layer.<sup>1-4</sup>

The roller charging, single-component development and toner transfer processes in EP share a common configuration shown in Fig. 1.<sup>2-4</sup> This prototype of rolls/belts system consists of a layer of semi-insulating dielectric on the conductive substrate, and an insulator layer (photoreceptor, toner-layer, air-gap), connected in series with a constant bias voltage  $V_B$ .

We shall first apply the conventional treatment of dielectric relaxation, namely the equivalent-circuit model, to this configuration. The results will be compared with a novel treatment of the process from first principle charge transport theory. The non-Ohmic nature of the contacts and low charge mobility are taken into consideration. It is shown that the relaxation proceeds at much slower rate than that expected from the resistance and capacitance, based on the equivalent-circuit equations. As the print speed increases, the time for each of these EP processes shortens, and may not allow the overcoat layer to relax completely. This elucidates the reason for the shortcoming of using resistance as the figure of merit. It will be shown that for high speed EP applications, where time allotted for each process is limited, the transient characteristics and the spatial variation, rather than the steady-state values and area averages, should be considered as the figure of merit.

## Equivalent-Circuit Model of Relaxation

Referring to the prototype of rolls/belts system shown in Fig. 1, at the application of the bias voltage  $V_B$  ( $t = 0$ ), the voltages across each of the two layers  $V_D$  and  $V_I$ , are divided in inverse proportion to their capacitances,  $C_D$  and  $C_I$ . (The subscript D and I refer to dielectric layer and insulator, respectively).

Due to the semi-insulating (“leaky”) nature of the dielectric layer, the voltage  $V_D$  decreases with time, while the voltage  $V_I$  increases. This is known as “dielectric relaxation” of the dielectric layer. In the traditional treatment of this process by equivalent circuit equations, the dielectric is represented by a parallel circuit of a resistance  $R_D$  and capacitance  $C_D$ , and the insulator by a capacitance  $C_I$ . The configuration is a series combination of the two and the bias voltage source  $V_B$  as shown in Fig. 2.

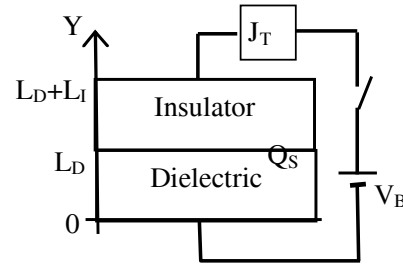


Figure 1. Schematic configuration for a prototype of rolls and belts in electrophotographic charging, development or transfer applications.

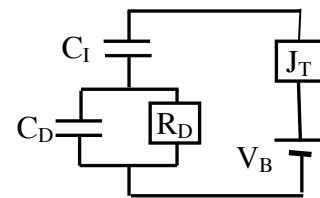


Figure 2. Equivalent circuit of the dielectric and insulator configuration shown in Figure 1.

The total current  $J_T(t)$  through the circuit can be expressed as,

$$J_T(t) = C_D(dV_D/dt) + V_D/R_D = C_I(dV_I/dt) \quad (1)$$

with the boundary condition that:  $V_D + V_I = V_B$ , hence,

$$(dV_D/dt) + (dV_I/dt) = 0 \quad (2)$$

Solving these equivalent circuit equations, one has for the time dependence of the voltages and total current as,

$$V_D(t) = [V_B C_I / (C_D + C_I)] \exp(-t/\tau) \quad (3)$$

$$V_1(t) = V_B[1 - C_1 \exp(-t/\tau)/(C_D + C_1)] \quad (4)$$

$$J_T(t) = [V_B C_1^2 / \tau (C_D + C_1)] \exp(-t/\tau) \quad (5)$$

where the time constant is,  $\tau = R_D(C_D + C_1)$ .

According to these results, both the voltages and the current are expected to vary exponentially with a time constant  $\tau$ . However, experimental observations of either the voltage or the current in rolls or belts in EP applications have failed to show such exponential decay.<sup>1</sup> This raises a question in the usefulness of “resistance” in characterization of rolls/belts. A resistance is given by  $R = L/\sigma$ , where  $L$  is the layer thickness and  $\sigma$  is the conductivity. The latter is given by the product of charge mobility  $\mu$  and intrinsic charge density  $q_i$ ,  $\sigma = \mu q_i$ . Thus, both  $R$  and  $\sigma$  are the layer bulk properties, independent of the condition at the contact interface to the substrate. The resistance can be used to determine the current only if the contact interface supplies charges sufficient to maintain the intrinsic value  $q_i$ . Such an interface is known as Ohmic contacts. This does not always happen in many EP configurations. A familiar example is seen in the dual-layer photoreceptors. The charge-transport layer (CTL) has a very high resistance in the dark (the intrinsic value), and hence, negligible current flows. But under illumination, a large amount of (photogenerated) charges can be injected from the contact with the charge-generation layer. Then, a current much larger than that expected from its intrinsic resistance flows in CTL.

A similar situation can be in effect in dielectric relaxation of rolls and belts. The charge supply from the bias is independent of the intrinsic value. Instead, the injection current from this “non-Ohmic” contact is strongly dependent on the physical condition of the contact and the field at the contact.

### Charge Transport Model of Relaxation

To describe dielectric relaxation with non-Ohmic contacts, we start with first principle charge transport equations. The mathematical details for the (single-layer) closed-circuit and open-circuit modes are described in a previous publication.<sup>1</sup> A similar procedure for the multi-layer configuration of Fig. 1, is given below.

The motion of charges in the dielectric is described by the continuity equation for the positive (or negative) charge densities  $q_p$  (or  $q_n$ ), given by, (omitting the subscripts  $p$  and  $n$ ),

$$\partial q(y, t) / \partial t = -\partial J / \partial y = -(\partial / \partial y)(\mu q E) \quad (6)$$

where  $J(y, t) = \mu q E$  is the conduction current,  $\mu$  is the charge mobility and  $E(y, t)$  is the electric field in the dielectric layer. The conduction current is zero in the insulator. The injection current from the bias can be assumed as linearly proportional to the field  $E(0)$  at the substrate,  $y = 0$ , with the proportionality constant  $s$  specifying the injection strength,

$$J_p(0) = sE(0) \text{ if } E(0) > 0 \text{ or } J_n(0) = sE(0) \text{ if } E(0) < 0 \quad (7)$$

The field  $E(y, t)$  is related to the charge densities  $q_p$  and  $q_n$ , and the permittivity  $\epsilon$  by Poisson's equation. The field discontinuity at the interface  $y = L_D$  is given by Gauss' theorem,

$$\epsilon_1 E_1 - \epsilon_D E_D(L_D) = Q_S(t) \quad (8)$$

where  $Q_S$  is the charge accumulated at the interface.

The voltages  $V_D$  and  $V_I$  in each layer are given by the integrals of fields, with the boundary condition that the sum is constant and equal to the bias voltage :  $V_D + V_I = V_B$ .

At  $t = 0$ , the charge-neutral conditions ( $q_p = -q_n = q_i$  and  $Q_S = 0$ ) yield the initial values of fields (uniform in each layer) as,

$$E_D = -V_B / \epsilon_D (L_D / \epsilon_D + L_I / \epsilon_I), \quad E_I = -V_B / \epsilon_I (L_D / \epsilon_D + L_I / \epsilon_I) \quad (9)$$

Starting from these initial conditions, the above set of equations can be solved by numerical iteration. Numerical examples of results are presented and discussed in the following.

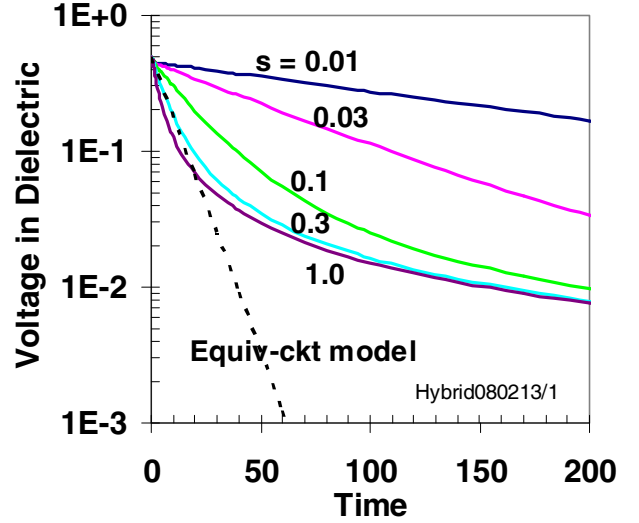


**Figure 3.** Solid curves: Decay of voltage  $V_D$  across dielectric layer of Fig. 1, with different charge injection strength  $s$ . Dashed curve shows the voltage decay expected from the equivalent circuit model.

**Table I. Normalized units**

Units	Typical Values
Length: $L_o$	$10^{-2}$ cm
Permittivity: $\epsilon_o$	$5 \times 10^{-13}$ F/cm
Voltage: $V_o$	$5 \times 10^2$ V
Charge mobility: $\mu_o$	$10^{-5}$ cm <sup>2</sup> /Vsec

Field: $E_o = V_o / L_o$	$5 \times 10^4$ V/cm
Time: $t_o = L_o / \mu_o E_o = L_o^2 / \mu_o V_o$	$2 \times 10^{-2}$ sec
Charge density / area: $Q_o = \epsilon_o E_o$	$2.5 \times 10^{-8}$ Coul/cm <sup>2</sup>
Charge density / vol.: $q_o = Q_o / L_o$	$2.5 \times 10^{-6}$ Coul/cm <sup>3</sup>
Injection strength: $s_o = \mu_o q_o$	$2.5 \times 10^{-11}$ S/cm

Figure 3 shows the time dependence of voltage across the dielectric layer, calculated with different injection strengths  $s$  (defined in Eq. 7). The intrinsic charge density  $q_i$  and charge mobilities,  $\mu_p$  and  $\mu_n$ , and hence the resistance have the same values in all cases. In spite of this, the voltages decay faster with larger injection strength  $s$ . But all decays are slower than the exponential one expected from the equivalent circuit model (Eq.3),

shown by the dashed line. It is this dependence on charge injection, and not the resistance, that controls the rate of dielectric relaxation in rolls and belts for various EP process.

The units used in this figure are normalized as listed in Table I. The curves in Fig.3 are calculated with  $V_B$ ,  $L_D$ ,  $\epsilon_D$ ,  $\mu_p$  and  $\mu_n$  having the unit values in the table, but  $L_l = 0.5$ ,  $\epsilon_l = 0.5$ , and the intrinsic charge density  $q_i = 0.1$ . However, the above conclusions are independent of these parameter values within the ranges of practical interest.

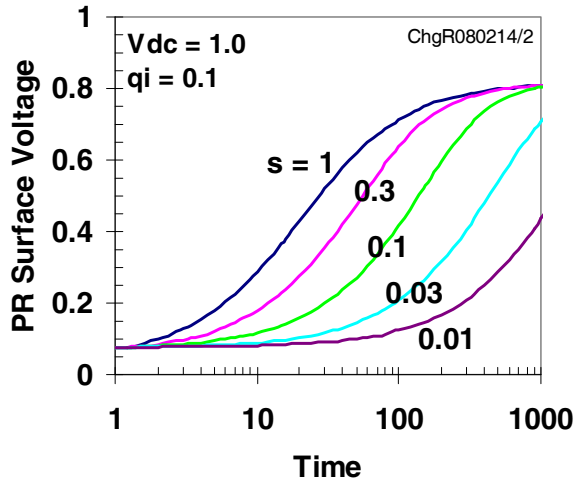


Figure 4. Growth of photoreceptor surface voltage by roll charging. The dependence on the strength of charge injection  $s$  is illustrated.

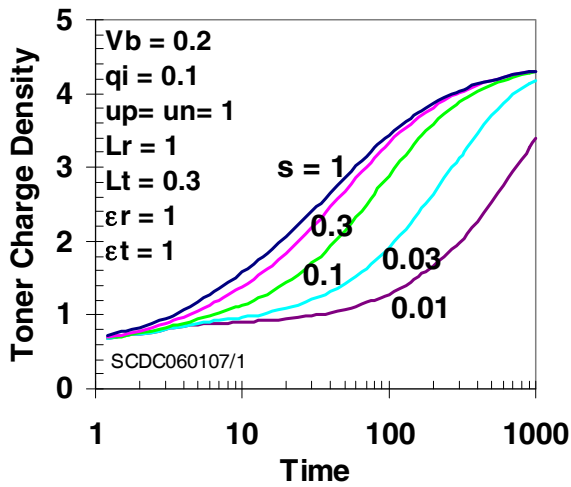


Figure 5. Growth of toner charge density at metering blade in single-component development, for various injection strengths  $s$ .

### Dielectric Relaxation in EP Processes

The key mechanism of dielectric relaxation in roll charging of photoreceptor, single-component development and electrostatic transfer can be analyzed with similar mathematical procedure as given above. Detailed discussions for these processes can be found in previous publications.<sup>2-4</sup> In this section, representative examples from each process are presented for further discussion.

Figure 4 shows an example of the growth of photoreceptor surface voltage with (roll) charging time.<sup>2</sup> The growth with time of toner charging and toner deposition efficiency in single-component development are shown in Figs. 5 and 6, respectively.<sup>3</sup> The deposition efficiency in Fig. 6 is defined as the ratio of toner-layer thickness where the field is in the direction of moving toners toward photoreceptor to the total toner-layer thickness. In Fig. 7, the growth of transfer field at the photoreceptor/toner-layer interface (in the direction of moving toners away from photoreceptor) is shown.<sup>4</sup>

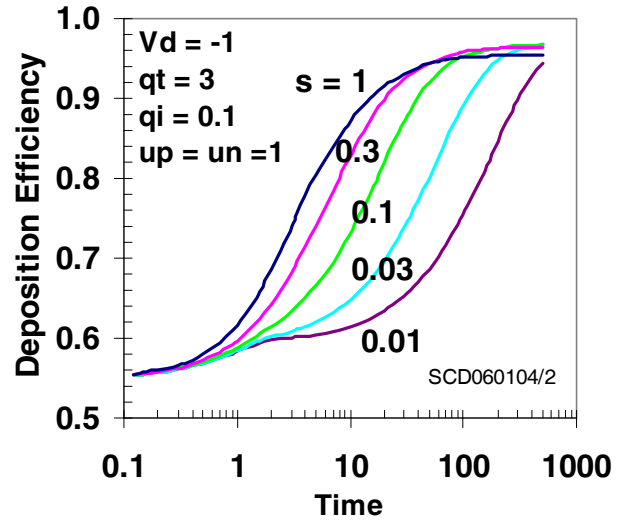


Figure 6. Increases of toner deposition efficiency with time, in single-component development, as injection parameter  $s$  varies.

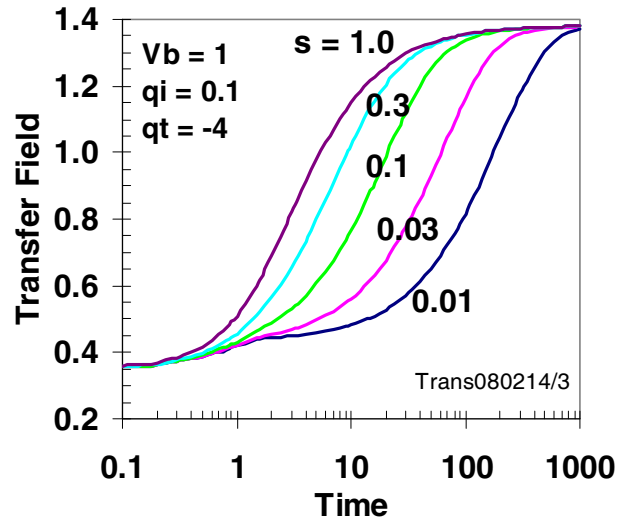
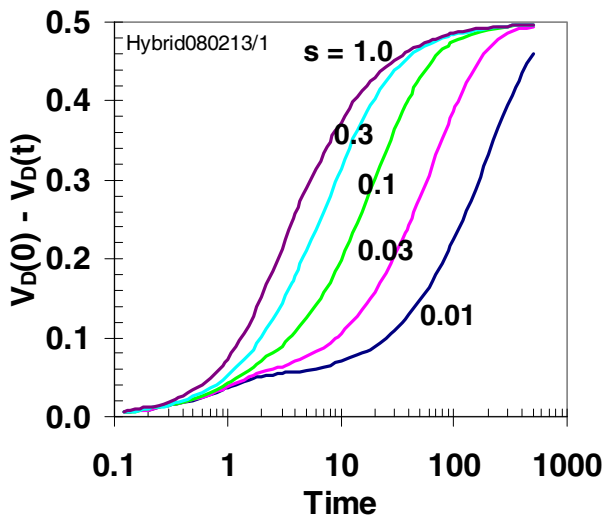


Figure 7. Growth of transfer field with time in electrostatic transfer, for different values of injection strength  $s$ .

## Discussion

A common feature in all of these figures (Figs. 4 -7) is that the performance parameters (in ordinates) seem to reach the same asymptotic values after long process time ( $> 1000t_0$ ), independent of the strength of charge injection  $s$  at the interface between the biased conductive substrate and the semi-insulating dielectric. However, there is strong dependence on  $s$  in the time range of a few tens to a few hundreds time units.

Returning to the prototype rolls and belts of Fig. 1, we re-plot the data of Fig. 3 as the voltage decay (or the extent of relaxation),  $V_D(0) - V_D(t)$ , versus time (in log scale). This is shown in Fig.8. Much resemblance in the dependence on injection strength and time can be seen between this figure and Figs. 4 to 7. This is a strong indication that the progress of these EP processes is closely related to the dielectric relaxation of the semi-insulating dielectric layer.



**Figure 8.** Voltage decay of prototype rolls/belts (Fig.3) re-plotted to show dependence on time and injection strength  $s$  of the voltage decayed in time  $t$ .

The dielectric layer is generally made of heterogeneous composite polymers. The spatial uniformity of electronic properties unlikely reaches the microscopic (pixel-size) scale. The results shown in Figs. 4-8 indicate that to avoid manifestation of spatial fluctuation in injection strength in a given sample, or sample-to-sample fluctuations, the time allotted for the relaxation in each process should be more than a few hundred time units.

In these figures, the unit of time (see Table I) is the nominal transit time, defined in terms of the layer thickness  $L_0$ , charge mobility  $\mu_0$ , and bias voltage  $V_0$  as,  $t_0 = L_0^2/\mu_0 V_0$ . With the typical values for EP applications (given in Table I), the time unit has a value of  $t_0 = 20$  msec. The data on Figs. 4-8 indicate that it requires over  $100t_0$  for the relaxation to become nearly independent of charge injection strength for  $s > 0.01$  unit. (see Table I for this unit). This means that in order to avoid the spatial and/or sample-to-sample fluctuations of injection strengths, the time allotted for the process (charging, deposition, or transfer) should be of the order of a second or longer. Assuming a nip width of the order of 1 mm, the process speed would be limited to

the order of 1 mm/sec or less. This is much smaller than the print speed desired today ( $> \approx 250$  mm/sec  $\approx 1$  page/sec). This means that the EP processes do not allow time for the layer to relax completely and to reach the final uniform state.

It should be noted that the time unit  $t_0$  varies quadratic in the layer thickness  $L_0$  (Table I). The above mentioned value of time unit  $t_0$  ( $\approx 20$  msec) is based on the assumption of  $L_0 \approx 100$   $\mu$ m. If the layer thickness is reduced by an order of magnitude, the time unit is reduced to 0.2 msec, and the print-speed limit can be raised to the order of 100 mm/sec, approaching that desired today.

Another way to overcome this limitation is to shorten the unit  $t_0$  (and the relaxation time) by increasing the charge mobility. However, not much information on the charge mobility in these materials, nor the way to increase it, is available today.

In conclusion, an ideal electrical characterization of rolls and belts for EP application should detect the microscopic (pixel-size) spatial variation in dielectric relaxation, manifested within time limits of high speed printing applications. It is not sufficient to observe the fully relaxed state after a time long compared to the practical process time. Since the dielectric relaxation is induced mainly by charge injection, the ideal characterization technique should include direct measurements of charge injection strength.

In the Electrostatic Charge Decay (ECD) technique for electrical characterization of rolls and belts,<sup>5</sup> the dielectric relaxation of the semi-insulator overcoat layer is monitored by measuring the open-circuit voltage decay of corona charged surface. This type of measurements simulates more closely the actual EP processes than the closed circuit resistance measurements. Furthermore, by scanning the corona charger and surface voltage detector over the roller/belt surface, the technique is capable of monitoring the transient spatial fluctuation non-destructively.

## References

- [1] I. Chen and M.-K. Tse, *J. Imaging. Sci. Technol.* **44**, 462, (2000)
- [2] I. Chen and M.-K. Tse, Proc. IS&T's NIP-21, pg. 566 (2005)
- [3] I. Chen and M.-K. Tse, Proc. IS&T's NIP-22, pg. 406 (2006)
- [4] I. Chen and M.-K. Tse, Proc. IS&T's NIP-20, pg. 30 (2004)
- [5] M.-K. Tse and I. Chen, Proc. Japan Hardcopy, pg.199 (2005)

## Author Biography

*Dr. Ming-Kai Tse is the founder and president of Quality Engineering Associates (QEA), Inc. in Burlington, MA, USA. Prior to founding QEA, Dr. Tse was an Associate Professor of Mechanical Engineering at the Massachusetts Institute of Technology (MIT). His research interest is in measurement technology, with special application in digital printing and image quality analysis. He earned his BS at Cornell University and his SM and PhD at MIT. He is a Senior Member of IS&T. He can be reached at mingkaitse@qea.com or 1-781-221-0080.*